Deciphering the monocyte-targeting mechanisms of PEGylated cationic liposomes by investigating the biomolecular corona

Münter, Rasmus; Bak, Martin; Thomsen, Mikkel E.; Parhamifar, Ladan; Stensballe, Allan; Simonsen, Jens B.; Kristensen, Kasper; Andresen, Thomas L.

Published in:
International Journal of Pharmaceutics

Link to article, DOI:
10.1016/j.ijpharm.2024.124129

Publication date:
2024

Document Version
Publisher's PDF, also known as Version of record

International Journal of Pharmaceutics 657 (2024) 124129

Contents lists available at ScienceDirect

International Journal of Pharmaceutics

journal homepage: www.elsevier.com/locate/ijpharm

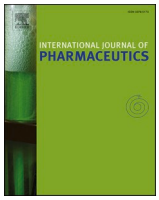

Deciphering the monocyte-targeting mechanisms of PEGylated cationic liposomes by investigating the biomolecular corona

Rasmus Münter [a], Martin Bak [a], Mikkel E. Thomsen [b], Ladan Parhamifar [a], Allan Stensballe [b,c], Jens B. Simonsen [a], Kasper Kristensen [a,*], Thomas L. Andresen [a,*]

[a] Biotherapeutic Engineering and Drug Targeting, Department of Health Technology, Technical University of Denmark, 2800 Kgs. Lyngby, Denmark
[b] Department of Health Science and Technology, Aalborg University, 9260 Gistrup, Denmark
[c] Clinical Cancer Center, Aalborg University Hospital, 9000 Aalborg, Denmark

ARTICLE INFO

Keywords:
Cationic liposomes
Biomolecular corona
Monocyte targeting
Drug delivery
Opsonins
Proteoglycans
Hyaluronan

ABSTRACT

Cationic liposomes specifically target monocytes in blood, rendering them promising drug-delivery tools for cancer immunotherapy, vaccines, and therapies for monocytic leukaemia. The mechanism behind this monocyte targeting ability is, however, not understood, but may involve plasma proteins adsorbed on the liposomal surfaces. To shed light on this, we investigated the biomolecular corona of three different types of PEGylated cationic liposomes, finding all of them to adsorb hyaluronan-associated proteins and proteoglycans upon incubation in human blood plasma. This prompted us to study the role of the TLR4 co-receptors CD44 and CD14, both involved in signalling and uptake pathways of proteoglycans and glycosaminoglycans. We found that separate inhibition of each of these receptors hampered the monocyte uptake of the liposomes in whole human blood. Based on clues from the biomolecular corona, we have thus identified two receptors involved in the targeting and uptake of cationic liposomes in monocytes, in turn suggesting that certain proteoglycans and glycosaminoglycans may serve as monocyte-targeting opsonins. This mechanistic knowledge may pave the way for rational design of future monocyte-targeting drug-delivery platforms.

1. Introduction

Cationic liposomes are promising delivery vehicles for targeted drug delivery (Dow, 2008; Lonez et al., 2008). They are easy to produce on a large scale and capable of carrying cargoes of both hydrophilic and hydrophobic drugs. Moreover, their positive surface charge facilitates cellular internalisation, thereby allowing for intracellular drug delivery (Bozzuto and Molinari, 2015; Dow, 2008; Mallick and Choi, 2014; Ramana et al., 2012). This is, for example, an essential requirement for delivery of agonists to intracellular receptors such as TLR3, 7, 8 and 9 for immunotherapy (Dow, 2008; Dowling, 2018; Javaid et al., 2019; Smits et al., 2008), or for delivery of nucleic acids for gene silencing and transfection (Akinc et al., 2019; Ruozi et al., 2003).

Cationic liposomes are readily recognised by cells of the mononuclear phagocyte system (MPS), e.g. macrophages, monocytes and neutrophils, and cleared rapidly from circulation (Blanco et al., 2015; Li and Szoka, 2007). On one hand, this may limit the ability of the liposomes to reach cells that are not part of the MPS, but on the other hand, this may create an opportunity to target certain cells of the MPS (de Lázaro and Mooney, 2021). To explore this opportunity, the interactions of cationic liposomes with circulating cells of the MPS were recently investigated, finding the liposomes to be specifically taken up by monocytes (Johansen et al., 2015; Münter et al., 2022a). Monocytes are present in blood in much higher numbers than dendritic cells and are more accessible than tissue-resident dendritic cells, thus making them attractive for both classical vaccination as well as for cancer immunotherapy (Karathanasis et al., 2009; Kelly et al., 2011; Klauber et al., 2017). Furthermore, as monocytes can differentiate into macrophages and enter tissues, monocytes could be targets for controlling the M1/M2 phenotype of macrophages resident in tumours (Guerriero, 2018) and atherosclerotic plaques (Bi et al., 2019; Bobryshev et al., 2016) as well as in rheumatoid arthritis (Fukui et al., 2018). Finally, monocytes are implicated in monocytic leukaemias (Shaw, 1980). Overall, the ability of cationic liposomes to specifically target monocytes and be internalised may thus lead to new avenues for treating a range of different diseases.

To guide the design of monocyte-targeting cationic liposome

* Corresponding authors.
E-mail addresses: kakri@dtu.dk (K. Kristensen), tlan@dtu.dk (T.L. Andresen).

https://doi.org/10.1016/j.ijpharm.2024.124129
Received 2 January 2024; Received in revised form 4 April 2024; Accepted 13 April 2024
Available online 14 April 2024

formulations and ensure a proper basis for their clinical translation, a thorough understanding of their mechanisms of targeting and uptake is essential. It has been suggested that plasma proteins adsorbed onto the surface of liposomes, forming a so-called biomolecular corona, govern the interactions between liposomes and biological systems, such as cells and tissue (Ong et al., 2021; Walkey and Chan, 2012). Inspired by this, we here analysed the biomolecular corona on three different types of PEGylated cationic liposomes in human blood plasma for the purpose of identifying biomolecules involved in the monocyte-targeting mechanisms of the liposomes. Our results demonstrate that several hyaluronan-associated proteins and proteoglycans are enriched in the biomolecular corona of the cationic liposomes. These proteins and their associated glycosaminoglycans interact with the TLR4 co-receptors CD44 and CD14 (Harris and Weigel, 2009; Kawashima et al., 2000; Shao et al., 2012), which are known to be involved in phagocytosis (Vachon et al., 2006). In the case of CD14, this receptor is known to be expressed to a higher degree on monocytes than on other leukocytes, also making it a classical monocyte marker (Schütt, 1999). Interestingly, CD14 has recently been shown to be involved the monocyte targeting of liposomes functionalized with cationic peptides (Münter et al., 2022a). To investigate the role of CD44 and CD14 in the monocyte targeting of cationic liposomes, we performed experiments in whole human blood, finding that separate inhibition of each of the receptors led to a profound decrease in the monocyte targeting of the cationic liposomes. We have thus identified that these two receptors are generally involved in the uptake of cationic liposomes by monocytes, in turn suggesting that proteoglycans and/or their associated glycosaminoglycans may function as opsonins and mediate monocyte targeting of the liposomes. This mechanistic knowledge may provide an important foundation for development of new and improved monocyte-targeting drug-delivery systems.

2. Materials and methods

2.1. Materials

All chemicals were acquired from Sigma-Aldrich (St. Louis, MO, US) unless otherwise stated. 1- Palmitoyl-2-oleoyl-*sn*-glycero-3-phosphocholine (POPC) and cholesterol were acquired from Lipoid (Ludwigshafen, Germany). 1-Palmitoyl-2-oleoyl-*sn*-glycero-3-phospho-(1′-*rac*-glycerol) sodium salt (POPG), 1-palmitoyl-2-oleoyl-*sn*-glycero-3-ethylphosphocholine chloride salt (POEPC), 1,2-dioleoyl-3-trimethylammonium-propane chloride salt (DOTAP) and 1,2-dioleoyl-*sn*-glycero-3-phospho-ethanolamine-N-[methoxy(polyethylene glycol)-2000] ammonium salt (DOPE-PEG2000) were acquired from Avanti Polar Lipids (Alabaster, AL, US). DOPE-Atto488 was acquired from ATTO-TEC (Siegen, Germany). 3,3′-Dioctadecyloxacarbocyanine perchlorate (DiO), and Hermes-1 and IM7 antibodies against CD44 were acquired from Thermo Fisher Scientific (Waltham, MA, US). The rat IgG2b clone RTK4530 and a FITC labelled version of IM7 for CD44 staining were acquired from Biolegend (San Diego, CA, US). Primary allophycocyanin-labelled CD14 antibodies for flow cytometry were acquired from BD Biosciences (Becton Dickinson, Franklin Lakes, NJ, US). Anti-CD14 (clone 18D11), CD36 blocking antibody (FA6-152) and control antibody (MOPC-21) was from Hycult Biotech (Uden, Netherlands). A linear version of the 4W9A peptide was acquired from Tocris/Bio-Techne (Abingdon, UK). Sodium hyaluronate with different molecular weights (5, 10, 25, 50, 500 kDa) were acquired from Lifecore Biomedical (Chaska, MN, US). 20-kDa Hyaluronan-FITC was acquired from Creative PEGWorks (Durham, NC, US). The TriArg lipopeptide (Cholesterol-GWRRR) and the 4W9A peptide was synthesized as previously described (Münter et al., 2022a).

2.2. Blood collection and plasma preparation

Whole human blood was drawn by certified staff from healthy donors under signed consent. The identities of the donors were unknown to the researchers performing the experiments. Unless otherwise stated, blood was always collected in hirudin tubes (Sarstedt, Nürnbrecht, Germany). All requirements for blood collection at the Technical University of Denmark were followed in agreement with the guidelines of the National Committee on Health Research Ethics. To prepare plasma, the blood was transferred to 2-mL Protein LoBind tubes (Eppendorf, Hamburg, Germany) and centrifuged at 3000*g* for 15 min in order to separate cells from plasma. The plasma supernatant was transferred to new Protein LoBind tubes and stored at 4 °C. The protein concentration in human plasma prepared using a similar method was approx. 80 mg/mL (Kristensen et al., 2021). Experiments with human plasma were always carried out on the same day as the blood was drawn.

2.3. Liposome preparation and characterisation

Lipids in powder forms were dissolved in *tert*-butanol:MQ water 9:1, mixed to the desired lipid compositions in glass vials and freeze-dried overnight. The dry lipids were hydrated in Dulbecco's PBS (without $CaCl_2$ and $MgCl_2$) to a concentration of 50 mM total lipid and put under 65 °C heating and magnet stirring for minimum 1 h. The size of the liposomes was controlled by extruding 21 times through a 100-nm Whatman filter (GE Healthcare, Little Chalfont, UK) using an Avanti mini-extruder (Avanti Polar Lipids) on a heating block at 45 °C. The liposomes were transferred to a new glass vial and stored at 4 °C. Total lipid concentration of the liposome stocks was determined by measuring the phosphorus concentration using ICP-MS. Samples were diluted 10,000 times in an ICP-MS diluent (2 % HCl, 10 ppb Ga) to fall within a standard range of 25–100 ppb phosphorus, and the phosphorus content was measured on an ICAP-Q from Thermo Fisher Scientific. The lipid concentration was calculated based on the assumption that 61.8 % of the lipids in our formulations contain a phosphorus atom, and after subtracting phosphorus background from the PBS. The hydrodynamic diameter and polydispersity index (PDI) of the liposomes were measured by dynamic light scattering (DLS) using a ZetaSizer Nano ZS from Malvern Instruments (Malvern, UK), equipped with a 633 nm laser. The liposomes were diluted to about 120 μM total lipid in PBS and the size measured as the average from 3 runs of 15 cycles. The zeta potential of the liposomes was measured using the same instrument by mixed measurement mode phase analysis light scattering (M3-PALS) in glucose buffer (300 mM glucose, 10 mM HEPES, 1 mM $CaCl_2$ at pH 7.4) at 120 μM total lipid. Each measurement consisted of 3 individual runs in automatic mode (10–100 cycles).

2.4. Leukocyte-uptake studies with flow cytometry

Whole human blood was obtained from healthy volunteers under signed content and collected in hirudin tubes. The blood was transferred to Protein LoBind tubes containing liposomes pre-diluted in RPMI, giving a final liposome concentration of 200 μM total lipid. The volume percentage of blood in the tubes was always kept above 80 %. The tubes were incubated for 60 min at 37 °C with 5 % CO_2 under rotation. After incubation of blood with liposomes, cells were washed three times in PBS containing 1 % FBS. In the experiments testing if liposomes were internalised or surface-associated, samples were instead washed three times in ice-cold PBS with 0.1 mg/mL (50 unit/mL) heparin. In between each wash, cells were centrifuged at 200*g* for 5 min and the supernatant discarded. Erythrocytes were lysed using PharmLyse lysis buffer (BD Biosciences). Four mL lysis buffer was added per 200 μL blood, followed by 15 min incubation in dark at RT. After centrifugation at 200*g* for 5 min and removal of supernatant, a second lysis with 1 mL lysis buffer for 5 min was done. Cells were washed twice in cold PBS containing 1 % FBS to stop the lysis. Human IgG was added to a concentration of 2 μg/10^6 cells to block unspecific binding and incubated on ice for 10 min before transferring to a Nunc round-bottomed 96 well plate (Thermo Fischer Scientific). Ten μL of allophycocyanin pre-conjugated CD14 specific

antibodies was added to stain monocytes and incubated on ice and in dark for 30 min. No CD14 staining was done in the experiments where CD14 had already been blocked with antibodies (see Section 2.9). The plate was spun for 8 min at 400*g* and washed with PBS twice. Finally, cells were resuspended in 100 µL PBS. Flow cytometry was performed using an ACCURI C6 flow cytometer (BD Biosciences), where 100,000 events were acquired on medium flow rate. Only events with a FSC-H signal above 1.2 x 10^6 were acquired. Allophycocyanin fluorescence from the CD14 staining was measured by exciting at 640 nm and detecting at 675/25 nm (FL4). Single cells were gated in an FSC-A/FSC-H plot, and cell subsets were gated using allophycocyanin fluorescence and an SSC-A/FSC-A plot (see Supplementary Figure S1). The uptake of liposomes with cells was evaluated using DOPE-Atto488 emission measured at 533/30 nm with excitation at 488 nm (FL1). The same channel (FL1) was used to determine leukocyte association of FITC-hyaluronan. Analysis was done in the FlowJo software (FlowJo LCC, Ashland, OR, US).

2.5. Uptake studies in the absence or presence of plasma

Whole human blood was drawn from donors as in the regular leukocyte-uptake experiments (Section 2.4). The blood was then transferred to Protein LoBind tubes and centrifuged at 500*g* for 10 min to pellet cells. The cell pellet was resuspended in 37 °C RPMI medium, and the tube centrifuged at 500*g* for 10 min. Three such washing steps were carried out. Meanwhile, plasma was acquired as described above from the same donors donating the blood. To assess uptake of liposomes in the absence or presence of plasma, liposomes were diluted to 400 µM total lipid in RPMI medium or in plasma, respectively, and added to the washed blood cells to mimic a 50 % hematocrit. Uptake was determined with flow cytometry as described in Section 2.4.

2.6. Liposome aggregation assay with flow cytometry

Aggregation was probed as previously described (Münter et al., 2022a). Briefly, liposomes were diluted to 200 µM total lipid in either PBS or in 50 % fresh human plasma in a 96- well plate. The samples were then incubated for 30 min at 37 °C. Flow cytometry was performed using an ACCURI C6 flow cytometer, collecting 50 µL of all samples on slow flow rate. Only events with a FSC-H signal above 80,000 were acquired.

2.7. Size-exclusion chromatography (SEC) for isolation of liposome from plasma and protein corona analysis

In order to investigate the binding of plasma proteins to liposomes, Atto488-labelled liposomes were diluted in fresh human plasma to a final concentration of 2 mM total lipid and approx. plasma concentration of 95 %. As a control, plasma diluted in PBS was used. After 1 h incubation, 1 mL of each sample was applied to an SEC column. SEC was performed using a Sepharose CL-4B matrix packed in 50 × 1.5 cm Econo-Column glass chromatography columns purchased from Bio-Rad (Hercules, CA, US) with PBS as mobile phase. The flow was kept at 0.5 mL/min using a Masterflex peristaltic pump (Cole-Parmer, Vernon Hills, IL, US). The first 24 mL eluting from the column was allowed to run into the waste before initating collection of fractions. Then, 24 1-mL fractions were collected, before allowing the free plasma proteins to elute into the waste. The column was left to clean for 105 min before adding the next sample. For each collected fraction, 125 µL was loaded into a black 96-well plate and the liposome elution profile determined using the DOPE-Atto488 fluorescence (excitation at 500 nm and reading emission at 520 nm). The lipid concentration of the fractions was estimated by comparing the measured fluorescence intensity to that of standard liposome samples of known lipid concentration. The protein concentration in the samples was estimated by measuring the protein autofluorescence (excitation at 295 nm and reading emission at 345 nm) and comparing to that of bovine serum albumin standard samples. Fluorescence readout was done using a Spark multimode microplate reader (Tecan, Männedorf, Switzerland). For each SEC run, the fractions containing > 7.5 % of the total eluting Atto488 intensity were pooled and used for further analysis by LC-MS/MS.

2.8. Liquid chromatography-tandem mass spectrometry (LC-MS/MS) for determination of biomolecular corona composition

LC-MS/MS was used to identify and quantify proteins bound to the liposomes after separation of liposomes from plasma using SEC. The LC-MS/MS experiments were performed following a previously described procedure (Kristensen et al., 2021, 2019; Münter et al., 2022b) with modifications. We first mixed 250 µL of each pooled SEC sample with 250 µL lysis buffer (5 % sodium deoxycholate, 50 mM triethylammonium bicarbonate, pH 8.5) in Protein LoBind tubes. The samples were then incubated at 95 °C for 5 min for denaturation of the proteins. Subsequently, the samples were transferred to a Microcon-10 kDa centrifugal filter unit (Merck, Darmstadt, Germany) and centrifuged at 14,000*g* until the solvent had flown through the filter. After discarding the filtrate, the samples were reduced and alkylated by adding 200 µL 10 mM tris(2-carboxyethyl)phosphine, 50 mM 2-chloroacetamide in digestion buffer (0.5 % sodium deoxycholate, 50 mM triethylammonium bicarbonate, pH 8.5) and incubating for 30 min at 37 °C. This was followed by another centrifugation at 14,000*g* until the solvent had flown through the filter. The filtrate was discarded, and the samples were washed by adding 200 µL digestion buffer, followed by another centrifugation (14,000*g*). The inner spin filters were transferred to new collection tubes, and Pierce trypsin protease, MS grade (Thermo Scientific) in digestion buffer was added to the filters in a protein:trypsin mass ratio of 50:1. The samples were vortexed and incubated overnight at 37 °C to digest the proteins. The samples were next centrifuged at 14,000*g* until the protein digest had flown through the filters. To ensure complete recovery of the protein digest, 100 µL 50 mM triethylammonium bicarbonate, pH 8.5 buffer was added to the filters, and the filters were centrifuged at 14,000*g* until the buffer had flown through the filters and into the collection tubes. Next, ethyl acetate extraction was performed by adding 450 µL ethyl acetate and 7.5 µL trifluoroacetic acid (TFA) to all tubes. The tubes were vortexed and centrifuged at 14,000*g* for 5 min to obtain phase separation. The top organic phase, containing the sodium deoxycholate and phospholipids, was removed by pipette to get rid of the sodium deoxycholate. Additional 450 µL ethyl acetate was added to all samples, and the procedure was repeated, thus attaining the bottom phase containing the peptides only. Each sample was then dried in a vacuum centrifuge and resuspended in 30 µL 2 % CH_3CN, 0.1 % TFA, 0.1 % formic acid (FA) aqueous solution. The samples were vortexed, spun down using a minicentrifuge, and ultrasonicated for 2 min. Subsequently, the samples were spun down at 14,000*g*, 8 µL of the supernatant loaded into a 96-well plate and spiked with a total of 100 fmol MS Qual/Quant QC Mix, yielding a total volume of 10 µL, which was all injected. The samples were investigated in technical dublicate using a UPLC-nanoESI MS/MS setup consisting of a Dionex RSLC nanopump (Dionex RSLC 3500, Thermo Fisher Scientific) connected to a Q Exactive HF-X-Hybrid Quadrupole-Orbitrap mass spectrometer (Thermo Fisher Scientific). The peptide samples were loaded onto a C18 reversed-phase pre-column (Dionex Acclaim PepMap RSLC C18, 2 µm, 100 Å, 100 µm × 2 cm) and separated on a 50-cm analytical C18 Micro pillar array column (µPAC, PharmaFluidics, Gent, Belgium) at 30 °C with a constant flow rate of 0.75 µL/min. The mobile phases were (A) water with 2 % CH_3CN and 0.1 % FA and (B) CH_3CN with 0.1 % FA. The loading was done with 2 % B over 5 min. The separation was performed by a linear gradient from 8 % B to 30 % B over 35 min. A full MS scan in the mass range of m/z 375 to 1200 was acquired at a resolution of 120,000. The precursor ions were isolated using a quadrupole isolation window of m/z 1.6 and fragmented using higher-energy collision dissociation (HCD) with a normalised collision energy of 28. Fragmented ions were dynamically added to an exclusion list for 15 s. All acquired MS scans

were searched using default settings in MaxQuant/Andromeda 1.6.10.43 against a human core reference database (Swiss-Prot, proteins entries: 20.368, accessed 20/10–2019). Standard settings were employed with carbamidomethyl (C) as a static modification, and protein N-terminal acetylation, deamidation (NQ) and oxidation (M) as variable modifications. Protein identification was reported at a false detection rate of 1 %, with identification match between runs toggled on. The MaxQuant results were processed using Perseus 1.6.10.43. One or more unique peptides in at least one group were required for protein quantification using label-free relative quantification (LFQ). Proteins only identified by site as well as reverse peptides were removed from the results. Keratins were considered to be contaminants, and were also removed from the final list of proteins. Composition of the biomolecular corona of the individual samples was determined based on the iBAQ values (Schwanhäusser et al., 2011). For comparison across different samples, LFQ values were used (Bennike et al., 2016; Cox et al., 2014; Ju et al., 2020).

2.9. Inhibition studies

Whole human blood was pre-incubated in Protein LoBind tubes for 30 min at 37 °C with 5 % CO_2 under gentle rotation, with or without the given inhibitor. The complement system was inhibited using the compstatin analog 4W9A (Mallik et al., 2005; Münter et al., 2022a). A linear version of 4W9A, unable to form the disulphide bond necessary for creating the circular structure needed for the effect of the peptide, was used as control (Münter et al., 2022a). The peptides were diluted to 520 μM in RPMI and then diluted 1:17 in whole human blood for a final concentration of 30.6 μM. The CD14 pathway was inhibited using an anti-CD14 monoclonal antibody (clone 18D11). The antibody was diluted in PBS to 85 μg/mL and added 1:17 to whole human blood for a final concentration of 5 μg/mL. As a negative control, the IgG1 clone MOPC-21 was prepared in the same dilution. Also, pure PBS without antibody was used as negative control. The CD44 pathway was inhibited using anti-CD44 monoclonal antibodies, either clone IM7 or Hermes-1. Each antibody was diluted in PBS to 170 μg/mL and added 1:17 to whole human blood for a final concentration of 10 μg/mL. As a negative control, the rat IgG2b clone RTK4530 was prepared in the same dilution. Also, pure PBS without antibody was used as negative control. After pre-incubation with the various inhibitors, the blood was mixed with liposomes (pre-diluted in RPMI to reach a final concentration of 200 μM total lipid after adding blood) and incubated for 60 min at 37 °C with 5 % CO_2 under rotation. The dilutions of liposomes in RPMI were adjusted in order to have the exact same concentration of both blood and liposomes as in experiments without inhibitor. Cell isolation, staining, and flow cytometry was then performed as described in Section 2.4.

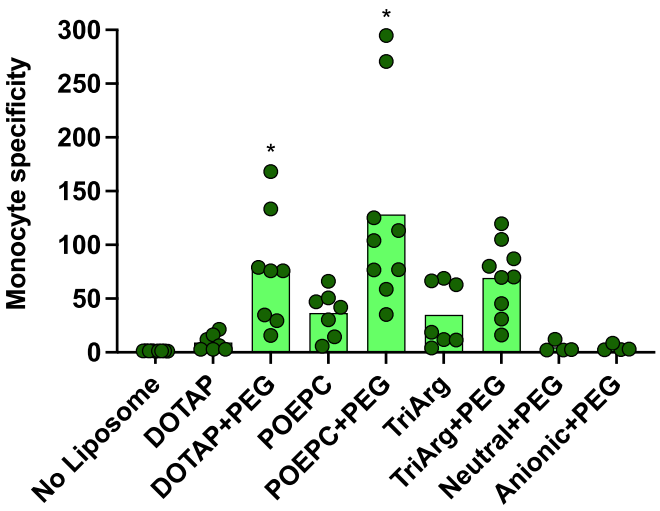

Fig. 2. Specificity of cationic liposomes to monocytes in whole human blood. The monocyte specificity was calculated by taking the ratio between the Atto488 MFI of the monocyte population and the Atto488 MFI of all other leukocytes. Each data point represents one donor, and the bars show the mean. Number of blood donors per group is the same as in Fig. 1. An asterix indicates that the monocyte specificity of a given type of liposome was significantly different from the monocyte specificity of PEGylated neutral liposomes ($p < 0.05$). Details about the statistical analysis, and exact p-values from this, can be found in Supplementary Table S3.

2.10. Statistical methods

Statistical analyses were performed using GraphPad Prism v10.0.0 (GraphPad Software, San Diego, CA, US). Error bars show standard deviation (SD) or standard error of the mean (SEM). Each data point corresponds to the readout from one blood donor, unless otherwise is specified. Association of liposome formulations to different cell populations (Fig. 1) were analyzed using a repeated measures two-way

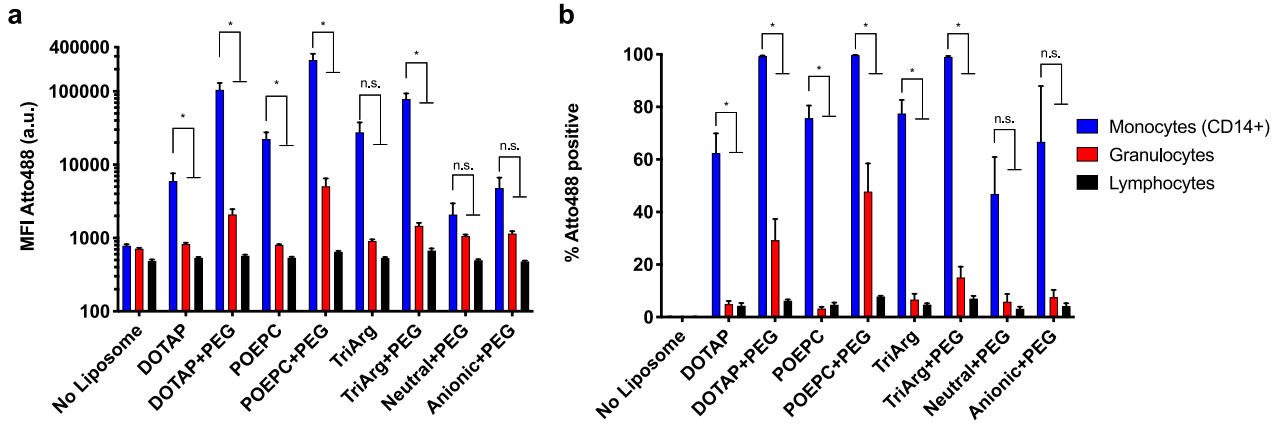

Fig. 1. Uptake of liposomes in peripheral blood leukocytes. Liposome uptake in leukocytes in whole human blood was assessed by flow cytometry. (a) Atto488 median fluorescence intensity (MFI) of the cells. (b) Percentage of Atto488 positive cells. Granulocytes and lymphocytes were gated based on morphology, and monocytes were gated based on both morphology and CD14 staining. Bars show mean, error bars show SEM. Number of blood donors per liposome group: n = 9 for No Liposome control, POEPC + PEG and TriArg + PEG; n = 8 for DOTAP + PEG; n = 7 for DOTAP, POEPC and TriArg; n = 4 for Neutral + PEG and Anionic + PEG. An asterix indicates statistical difference between the monocytes and the other cell populations ($p < 0.05$), "n.s." indicates no statistical difference. Details about the statistical analysis, and exact p-values of this, can be found in Supplementary Table S1 and S2.

ANOVA with Tukey's multiple comparison post hoc test with donor matching and Geisser-Greenhouse correction. To compare PEGylated and non-PEGylated liposomes, the data in Fig. 1 were also analyzed by multiple paired t-tests with Holm-Sidak's adjustment for multiple comparisons. For comparing monocyte specificity of various formulations (Fig. 2) a one-way ANOVA with Holm-Sidak's multiple comparisons post-hoc test and donor matching was used. Inhibition effects (Figs. 3 and 5 as well as associated Supplementary Figures) was analyzed using a two-way ANOVA: the specific post hoc tests for the individual experiments are described in the associated table legends of Supplementary Tables S4-S6. The results of all statistical analyses (and an explanation of the specific hypotheses being tested for) are listed in Supplementary Tables S1-S8, with references given to the relevant table in the individual figure caption.

3. Results and discussion

3.1. Liposome characteristics

We initially set out to study monocyte targeting with both non-PEGylated and PEGylated cationic liposomes. The liposomes were based on a POPC:cholesterol scaffold into which we incorporated one of three different cationic lipids: (i) DOTAP, which carries a positive charge due to a quaternary amine; (ii) ethyl-PC (POEPC), which is POPC with an ethyl group bound to a phosphate oxygen to remove a negative charge from the otherwise zwitterionic headgroup; or (iii) cholesterol-anchored triarginine (TriArg), which is based on the peptide sequence GWRRR, recently shown to confer monocyte-targeting properties on liposomes (Münter et al., 2022a). The PEGylated liposomes furthermore contained 5 % DOPE-PEG2000 (Table 1).

It has previously been found that optimal monocyte targeting is achieved for non-PEGylated liposomes having a zeta potential in the range 31–38 mV and for PEGylated liposomes having a zeta potential in the range 13–25 mV (Andresen et al., 2019; Johansen et al., 2015). To obtain this zeta potential, the non-PEGylated liposome were prepared with 7.5 % DOTAP, 7.5 % POEPC, or 2 % TriArg, and the PEGylated liposomes with 20 % DOTAP, 20 % POEPC, or 6 % TriArg. As shown in Table 1, the non-PEGylated liposomes all had a zeta potential of 35–38 mV, and the PEGylated of 17–19 mV. The size of the liposomes was approx. in the range 120–130 nm with a low polydispersity. For comparison, PEGylated liposomes with neutral or negatively charged surfaces were also prepared. For leukocyte-uptake experiments and tracing, 0.1 % of the fluorescently labelled lipid DOPE-Atto488 was added to all liposomes.

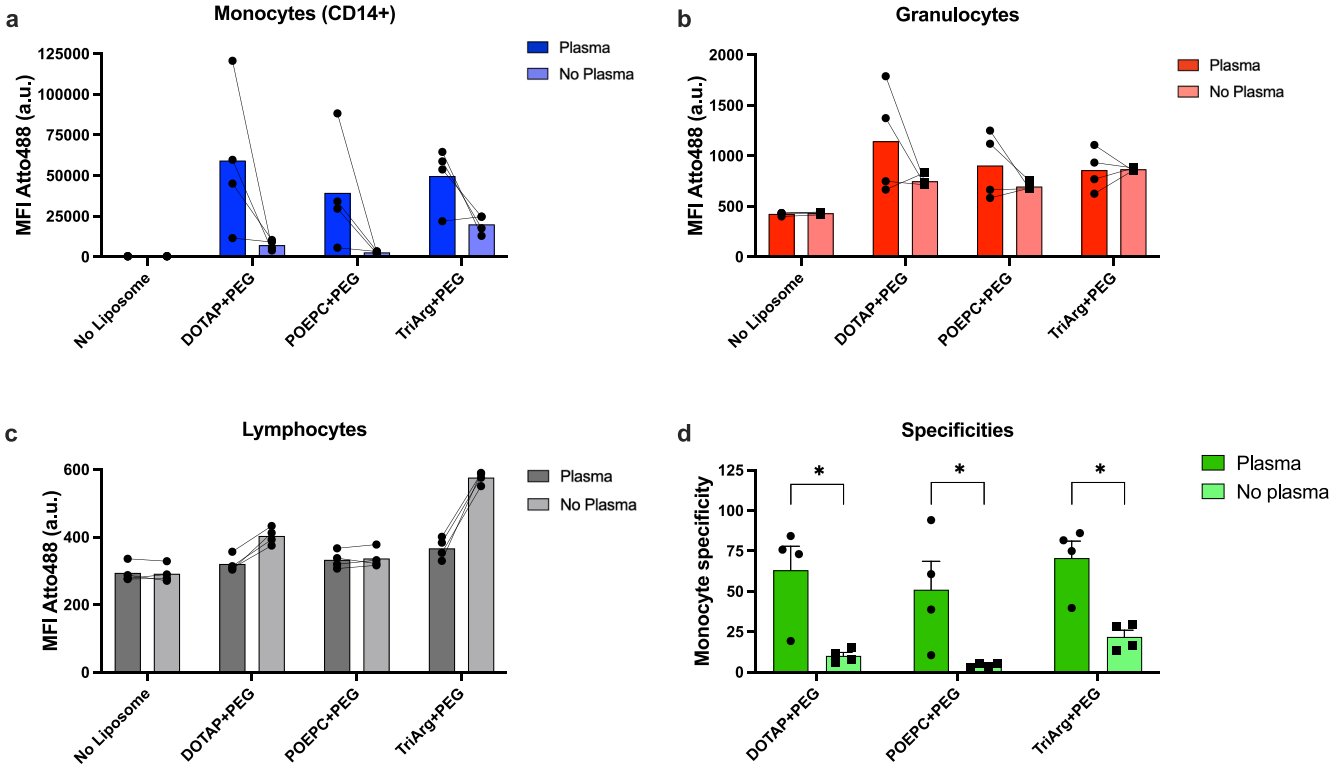

Fig. 3. Leukocyte uptake of cationic liposomes in absence of plasma. Blood cells were separated from plasma and resuspended in either serum-free RPMI medium or plasma from the same donor. The leukocyte uptake of the liposomes was then determined using flow cytometry. (a,b,c) MFI value of the Atto488 liposome label for monocytes (a), granulocytes (b) and lymphocytes (c) in absence or presence of plasma. The dots show the uptake for each individual donor, and the data points from the same donor are connected. (d) Monocyte specificity in absence or presence of plasma, calculated as the MFI of CD14 + monocytes compared to all other (CD14-) leukocytes. Bars show mean, error bars show SD. Number of blood donors included in the study was four for all types of liposomes. An asterix indicates statistical difference between the MFI value in presence of plasma or absence of plasma ($p < 0.05$). Details about the statistical analysis, and exact p-values from this, can be found in Supplementary Table S4 and S5.

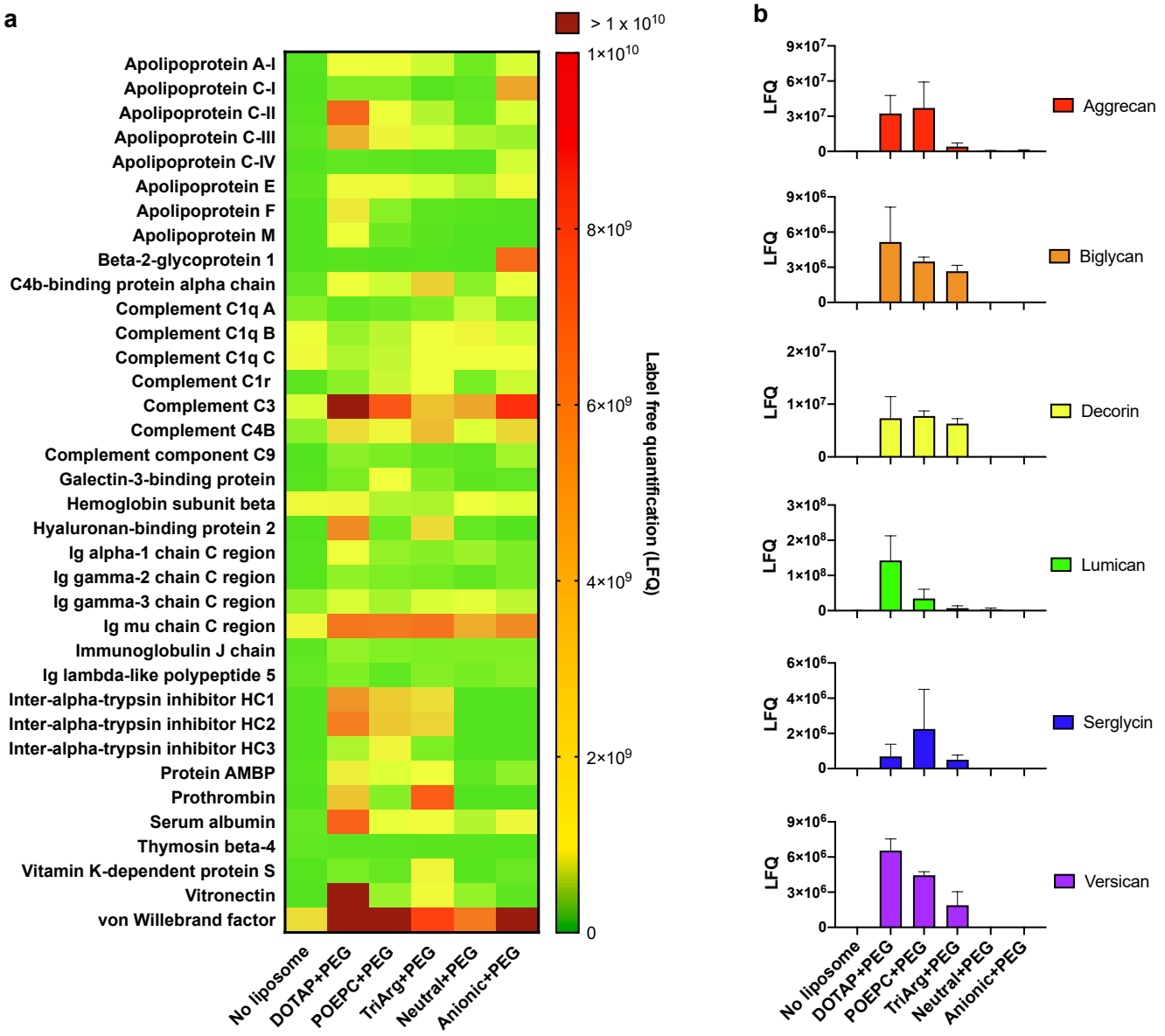

Fig. 4. Composition of the biomolecular corona of PEGylated liposomes. The liposomes were incubated in human plasma and subsequently isolated using size-exclusion chromatography. The 15 most abundant proteins in the biomolecular coronas of PEGylated cationic, neutral, and anionic liposomes in human plasma were identified using LC-MS/MS. (a) Label-free relative quantification (LFQ) value of each protein across the investigated liposome samples. (b) LFQ values of proteoglycans in the liposome samples. Data show mean values of samples from three different blood donors. Error bars show SEM.

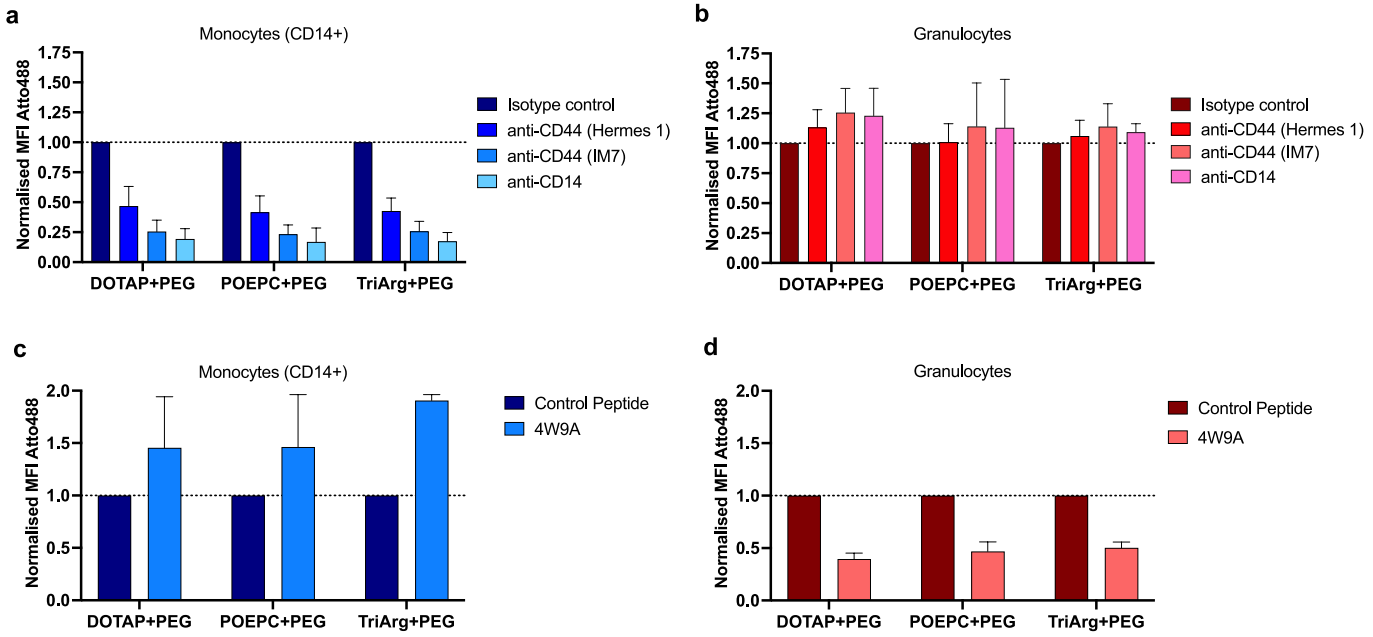

Fig. 5. Inhibition of leukocyte uptake with CD44 and CD14 blocking antibodies and complement inhibitor 4W9A. Whole human blood was treated with either blocking antibodies against CD44 (IM7 and Hermes-1 clones), blocking antibody against CD14, complement C3-inhibiting peptide analogue 4W9A, or appropriate isotype antibody or inactive peptide controls. PEGylated cationic liposomes were then added, and the uptake in leukocytes assessed with flow cytometry. (a) Atto488 MFI in monocytes upon treatment with blocking antibodies normalised to the Atto488 MFI in monocytes upon treatment with a non-specific isotype antibody. (b) Atto488 MFI in granulocytes upon treatment with blocking antibodies normalised to the Atto488 MFI in granulocytes upon treatment with a non-specific isotype antibody. (c) Atto488 MFI in monocytes upon treatment with the complement factor C3 inhibiting peptide 4W9A normalised to the Atto488 MFI in monocytes upon treatment with an inactive control peptide. (d) Atto488 MFI in granulocytes upon treatment with the complement factor C3 inhibiting peptide 4W9A normalised to the Atto488 MFI in granulocytes upon treatment with an inactive control peptide. Bars show mean, error bars show SD. The data represent experiments performed in blood from three different donors. Non-normalized data can be found in Supplementary Figure S19. A statistical analysis of those data can be found in Supplementary Table S6.

Table 1
Composition and characteristics of liposome formulations used in this study. The size and polydispersity index (PDI) were measured using dynamic light scattering, and the zeta potential was measured using mixed measurement mode phase analysis light scattering. All values are shown as the mean and standard deviation of 3–6 liposome batches. For leukocyte-association experiments and tracing, we added 0.1 % DOPE-Atto488 to the formulations.

Formulation	Composition (molar ratio)	Size (nm)	PDI	Zeta potential (mV)
DOTAP	POPC:DOTAP:cholesterol(62.5:7.5:30)	124.9 ± 14.8	0.123 ± 0.058	37.5 ± 0.8
DOTAP + PEG	POPC:DOTAP:cholesterol:DOPE-PEG (45:20:30:5)	127.8 ± 7.2	0.056 ± 0.017	17.0 ± 2.2
POEPC	POPC:POEPC:cholesterol(62.5:7.5:30)	128.2 ± 5.9	0.061 ± 0.054	34.5 ± 3.3
POEPC + PEG	POPC:POEPC:cholesterol:DOPE-PEG (45:20:30:5)	127.6 ± 9.7	0.053 ± 0.019	17.4 ± 2.0
TriArg	POPC:TriArg:cholesterol(68:2:30)	134.3 ± 7.3	0.082 ± 0.052	35.8 ± 3.9
TriArg + PEG	POPC:TriArg:cholesterol:DOPE-PEG (59:6:30:5)	131.6 ± 9.0	0.033 ± 0.017	19.2 ± 3.8
Neutral + PEG	POPC:cholesterol:DOPE-PEG (65:30:5)	125.8 ± 6.1	0.044 ± 0.021	−10.9 ± 5.4
Anionic + PEG	POPC:POPG:cholesterol:DOPE-PEG (45:20:30:5)	123.9 ± 6.3	0.041 ± 0.009	−13.5 ± 6.1

3.2. Cationic liposomes are preferentially taken up by monocytes

To confirm that the prepared cationic liposomes preferentially target monocytes, they were incubated in fresh whole human blood for 1 h, and the cellular uptake measured with flow cytometry after lysis of the red blood cells. The gating strategy for determining uptake in various subsets of blood leukocytes is shown in Supplementary Figure S1 and S2. The blood was prepared using the anticoagulant hirudin. One benefit of hirudin is that it is specific towards a single target, namely thrombin, in contrast to commonly used anticoagulants, such as citrate, EDTA and heparin, which act upon multiple targets, affect many biomolecular pathways and cells in the blood, and affect some types of biochemical assays (Bexborn et al., 2009; Cedrone et al., 2018). Since citrate, EDTA and heparin are all negatively charged, they may also lead to ionic screening of the cationic liposomes, which in turn may alter the interactions of the liposomes with both biomolecules (Schöttler et al., 2016) and cells (Supplementary Figure S3).

Using the described setup, we found that the cationic liposomes generally associated with monocytes over granulocytes and lymphocytes (Fig. 1). The PEGylated cationic liposomes displayed a higher association to the monocytes, but also a higher off-target association to the granulocytes than their non-PEGylated counterparts. There was some variability in the results between the individual donors, but the association to the monocytes was consistently higher than the association to the granulocytes for all types of cationic liposomes in all blood donors (Supplementary Figure S4 and S5). In agreement with earlier findings (Ong et al., 2021), non-charged liposomes also associated to monocytes. In comparison to the cationic liposomes, however, the PEGylated neutral and anionic liposomes displayed a much lower monocyte association, emphasising the importance of the positive charge for efficient monocyte targeting.

To assess whether the flow cytometry data reflected liposomal uptake and not solely association to the plasma membrane, the above experiments were repeated, but this time the cells were washed with 50 U/

mL heparin before performing the flow cytometry. Such washing steps have previously been demonstrated to efficiently remove non-internalised cationic liposomes (Iwasa et al., 2006; Korsholm et al., 2007). As shown in Supplementary Figure S6, the heparin washing did not lead to a decrease in the measured median fluorescence intensity (MFI). Thus, we concluded that the flow cytometry data in Fig. 1 reflected internalised liposomes.

To further evaluate the monocyte targeting of the investigated liposomes, we calculated their monocyte specificity, defined as the ratio between the MFI of the monocytes and the MFI of all other leukocytes. Doing this, we estimated a mean monocyte specificity of 9–36 for the three types of non-PEGylated cationic liposomes and 69–128 for the three types of PEGylated cationic liposomes (Fig. 2), although there were noteworthy variations in responsiveness of the donors. In comparison, the monocyte specificity for the PEGylated neutral and anionic liposomes was measured to be 5 and 4, respectively, although the actual specificity may have been somewhat higher than the calculated, since the uptake of these liposomes in the granulocytes and lymphocytes was so low that it may have been masked by the autofluorescence of the cells. When subtracting the autofluorescence from the measured Atto488 intensities and performing the specificity calculation on these adjusted MFI values, the average monocyte specificity of the neutral and anionic liposomes was 14 and 12, respectively (Supplementary Figure S7). In comparison, the cationic liposomes had mean specificities ranging from 64 to 838 for this type of calculation (though typically between 130 and 200). As there was notable liposome uptake in both monocytes and granulocytes (the two main phagocytic leukocyte populations in blood) but almost no uptake in lymphocytes, we also calculated the monocyte specificity defined as the ratio between the MFI of the monocytes and the MFI of the granulocytes specifically. The results from this analysis (Supplementary Figure S8) were similar to the results shown in Fig. 2.

To further probe the interaction of the cationic liposomes with the monocytes, we used the DNA-binding dye 7AAD to measure the cell viability. As shown in Supplementary Figure S9, the liposomes were generally non-toxic to blood cells. Significant toxicity was, however, observed for monocytes, albeit there were large differences in the results between individual donors. There was no clear difference in the toxicity of the different cationic liposomes. Optimization of the lipid composition or dosing of the liposomes may lead to reduced toxicity (Filion and Phillips, 1997; Knudsen et al., 2015), but it is still clear that cytotoxicity may represent a potential issue that needs to be solved if cationic liposomes are to be used clinically as monocyte-targeting platforms. Since the overall purpose of the present study was to elucidate the mechanisms that lead cationic liposomes to target monocytes, we did not consider the toxicity issue in further detail.

3.3. Non-PEGylated cationic liposomes aggregate in plasma

Plasma may influence the monocyte targeting of cationic liposomes in several ways. Certain liposomal formulations, for example, may aggregate in plasma affecting their propensity of being recognised and phagocytosed by immune cells (Ahl et al., 1997). We therefore went on to evaluate the aggregation of the liposomes in human plasma using flow cytometry (Supplementary Figure S10 and S11). The non-PEGylated cationic liposomes were found to aggregate in plasma, possibly because interactions between the cationic lipids and anionic plasma species led to charge neutralisation of the liposomal surfaces and/or bridging flocculation of the liposomes (Moore et al., 2015; Zhao et al., 2011). As such severe aggregation would have negative impact on the circulation properties and safety profile of the liposomes, the non-PEGylated cationic liposomes are unlikely to be clinically relevant for leukocyte targeting in blood; therefore, we decided to exclude these liposomes from the remainder of the experiments. Very few aggregates were, however, detectable for the PEGylated liposomes, indicating that these were more stable in plasma. This is in line with earlier results, showing that PEGylation increases the stability of liposomes in plasma (Allen et al., 2002; Münter et al., 2022a; Münter and Simonsen, 2023). As the leukocyte uptake of these liposomes was unaffected by aggregation, we went on to study if plasma proteins adsorbed onto the surface of the liposomes could explain their monocyte-targeting behaviour (Corbo et al., 2016).

3.4. Plasma is involved in monocyte targeting of cationic liposomes

Having confirmed that the cationic liposomes were specifically taken up by monocytes in whole human blood, we next wanted to investigate their monocyte-targeting mechanisms. As the plasma membrane of cells holds a negative surface charge (Nishino et al., 2020), cationic liposomes could in principle associate non-specifically to all leukocyte populations. As we did not observe such non-specific association, we hypothesised plasma factors to be responsible for the liposomes' monocyte specificity. To test this hypothesis, we separated blood cells from plasma by centrifugation and resuspended them in either serum-free RPMI medium or in plasma from the same donor. Cationic liposomes were then added and uptake in leukocytes investigated as described above. Fig. 3 shows the leukocyte uptake in the absence of plasma compared to the uptake in the presence of plasma. The absence of plasma caused a marked reduction in monocyte uptake for all liposomes in most donors, but only a modest decrease, and in some cases even an increase, in granulocyte and lymphocyte uptake. Reflecting this, the absence of plasma led to a significant decrease in the monocyte specificity of the liposomes (Fig. 3d; monocyte specificity compared to granulocytes can be found in Supplementary Figure S12). Overall, this supported the hypothesis of plasma factors being involved in the monocyte targeting of cationic liposomes.

3.5. Hyaluronan-associated proteins and proteoglycans are enriched in the biomolecular corona of PEGylated cationic liposomes

To characterise their biomolecular corona, the PEGylated cationic, neutral, and anionic liposomes were incubated in human plasma for 1 h. The liposomes were then separated from the soluble plasma proteins using size-exclusion chromatography (Supplementary Figure S13), and the proteins co-eluting with the liposomes were identified using liquid chromatography-tandem mass spectrometry (LC-MS/MS). For comparison, a liposome-free plasma sample was also included to analyse the background proteins co-eluting with the liposomes (Kristensen et al., 2021, 2019).

While there was substantial protein adsorption onto the cationic and anionic liposomes, in particular the DOTAP liposomes (Supplementary Figure S14), there was only modest protein adsorption onto the neutral liposomes. To identify proteins that could be relevant for the monocyte targeting of cationic liposomes, we compared the identity of the proteins in the biomolecular corona of the cationic liposomes to that of the neutral and anionic liposomes. The complete list of proteins identified with LC-MS/MS is shown in the Supplementary Data. The 15 most abundant proteins in each sample, representing 80–90 % of the total amount of protein, were ranked in abundance based on intensity based absolute quantification (iBAQ) values (Supplementary Figure S15), and their content compared across the samples based on the label-free relative quantification (LFQ) values (Fig. 4a; Ju et al., 2020). This revealed that complement C1q and hemoglobin were abundant in several of the liposomes samples, but it was questionable whether they adsorbed onto the liposomes as they were also abundant in the liposome-free samples (Kristensen et al., 2021, 2019). Complement C3 and C4B, IgM, serum albumin, von Willebrand factor, and several apolipoproteins, on the other hand, were abundantly represented in all of the liposome samples to a higher extent than in the liposome-free samples, implying them to constitute a significant part of the biomolecular corona of all of the investigated liposomes. The apolipoproteins were of particular interest since they are known to mediate cellular uptake of bionanoparticles, such as lipoproteins, and have also been implicated in

cellular uptake of lipid-based drug delivery vechicles (Akinc et al., 2010; Alam et al., 2023; Pedersbæk et al., 2020). However, since they were equally abundant in the corona of both cationic and anionic liposomes, we concluded that they were most likely not involved in the monocyte targeting of the cationic liposomes. Instead, we focused on the proteins specifically enriched in the biomolecular coronas around the cationic liposomes. Among the proteins shown in Fig. 4a, hyaluronan-binding protein 2 and inter-alpha-trypsin inhibitor – the latter represented by its heavy chains 1 and 2 as well as its light chain protein AMBP – were enriched in the samples with the cationic liposomes. Interestingly, both of these proteins are associated with the glycosaminoglycan hyaluronan (Fries and Kaczmarczyk, 2003; Zhuo and Kimata, 2008), suggesting this molecule to govern their adsorption to cationic liposomes. Indeed, hyaluronan-binding proteins have been found to mediate cellular uptake of gold nanoparticles (Walkey et al., 2014). Prompted by this observation, we went on to consider whether other glycosaminoglycan-associated proteins, particularly proteoglycans (proteins with covalently attached glycosaminoglycans), were enriched in the corona on the cationic liposomes. As shown in Fig. 4b, this was indeed the case for aggrecan, biglycan, decorin, lumican, serglycin, and versican. The reason for this enrichment of proteoglycans in the biomolecular corona of the cationic liposomes may be that the negatively charged glycosaminoglycans are electrostatically attracted to the positively charged liposome surfaces.

Based on the finding that hyaluronan-associated proteins and proteoglycans were highly abundant on monocyte-targeting cationic liposomes, but not on neutral and anionic liposomes, we went on to test if receptors recognising glycosaminoglycans and proteoglycans were involved in the monocyte uptake of cationic liposomes.

3.6. Monocyte targeting of cationic liposomes is governed by CD44 and CD14

Hyaluronan and proteoglycans are components of the extracellular matrix, in general serving adhesive and space-filling purposes (Frey et al., 2013; Petrey and de la Motte, 2014). Increased levels of low-molecular weight hyaluronan fragments and proteoglycans in the plasma is a sign of tissue damage, and are therefore recognised by TLR receptors as danger associated molecular patterns (DAMPs; Frey et al., 2013). The TLR4 co-receptor CD44, for example, is known to bind hyaluronan (Isacke and Yarwood, 2002; Underhill, 1992) and several proteoglycans, such as inter-alpha-trypsin inhibitor (Fries and Kaczmarczyk, 2003; McDonald and Kubes, 2015) and aggrecan (Danielson et al., 2015; Embry and Knudson, 2003; Fujimoto et al., 2001). Since the receptor is widely expressed on leukocytes (see Supplementary Figure S16) and known to be involved in phagocytosis (Goodison et al., 1999; Senbanjo and Chellaiah, 2017; Vachon et al., 2006), we hypothesised it to be involved in the leukocyte internalisation of cationic liposomes through recognition of hyaluronan and associated proteoglycans adsorbed on the liposomal surfaces. Further fuelling this hypothesis was the fact that hyaluronan itself specifically associated with monocytes, and that this association was increased in the presence of cationic liposomes (Supplementary Figure S17).

To investigate the involvement of CD44 in the monocyte targeting mechanism of PEGylated cationic liposomes, we incubated fresh whole human blood with blocking antibodies (clone IM7 or Hermes-1, see also Supplementary Figure S18) against CD44. After 30 min, the liposomes were added to the blood, and after 1 h of additional incubation, their leukocyte uptake was assessed by flow cytometry as described above. To confirm that the observed effects were specific for the blocking antibodies, the same experiments were performed with an isotype-matched antibody, not recognising the receptor. As illustrated in Fig. 5a, inhibition of CD44 resulted in decreased uptake in monocytes of all of the liposomes in all donors (non-normalized data for individual donors can be found in Supplementary Figure S19). The uptake in the granulocytes, on the other hand, was largely unaffected by the inhibition (Fig. 5b), resulting in a generally decreased monocyte specificity of the liposomes (Supplementary Figure S20). These results demonstrate that CD44 is involved in the monocyte-targeting mechanisms of cationic liposomes. The mechanisms are, however, not only related to the presence of hyaluronan, as we found that hyaluronan-coating of liposomes, with or without cationic lipids, did not increase monocyte specificity (Supplementary Figure S21 and S22). This either suggests that CD44 recognises proteoglycans or other glycosaminoglycans on the surface of the cationic liposomes, or alternatively, that the surface-adsorbed proteoglycans present hyaluronan with an optimal surface orientation for recognition by CD44. It may also be that the positively charged lipids play a role in the recognition and internalisation process.

The proteoglycan lumican, which was also enriched in the biomolecular coronas on the cationic liposomes, has been characterised as a lipopolysaccharide (LPS)-sensing protein, driving TLR4 signalling in response to LPS and mediating bacterial phagocytosis through the CD14 co-receptor (Shao et al., 2012; Wu et al., 2007). As CD14 is upregulated on monocytes (Schütt, 1999), and was found to be involved in monocyte targeting of liposomes functionalized with TriArg (Münter et al., 2022a), we investigated whether CD14 was involved in the monocyte targeting of cationic liposomes in general. Therefore, we repeated the blocking experiment described above, but this time with an antibody blocking CD14. As was the case for CD44, blockade of CD14 also resulted in decreased monocyte uptake for all liposomes in all donors (Fig. 5a and Supplementary Figure S19a), unaffected granulocyte uptake (Fig. 5b and Supplementary Figure S19b), and decreased monocyte specificity (Supplementary Figure S20) of the liposomes. Thus, CD14 is also involved in the monocyte-targeting mechanism of cationic liposomes, possibly mediated by lumican adsorbed to the liposomal surfaces.

Both CD44 and CD14 are co-receptors for the pattern recognition receptor TLR4, sensing the presence of DAMPs (Muto et al., 2009; Płóciennikowska et al., 2015). The scavenger receptor CD36 is also a co-receptor for TLR4, involved in phagocytosis of apoptotic cells and recognition of DAMPs (Fadok et al., 1998; Frey et al., 2013; Silverstein and Febbraio, 2009). As CD36 has been implicated in monocyte phagocytosis of both apoptotic cells (Fadok et al., 1998) and pathogens (Cao et al., 2016), we tested how blocking this receptor affected the leukocyte uptake of cationic liposomes as well, following the procedure described above. We found that inhibition of this receptor also resulted in a significant decrease in monocyte uptake of the liposomes (Supplementary Figure S23a), but as the decrease in uptake was associated with a decrease in monocyte count (Supplementary Figure S23b), this effect cannot be ascribed to inhibition of phagocytic processes only. Yet, it is highly interesting that CD44, CD14, and CD36 are all involved in the TLR4 axis (Cao et al., 2016; Ruffell et al., 2011; Stewart et al., 2010; Zanoni et al., 2011). Some signalling mechanisms through TLR4 have been demonstrated to necessitate the presence of both CD14 and CD44 in close vicinity (Horvatinovich et al., 2017), possibly suggesting that we have identified a common mechanism for monocyte targeting of cationic liposomes rather than several parallel mechanisms.

The complement system – part of the innate immune system – is one of the most well-investigated mechanisms involved in the clearance of liposomes (Ishida et al., 2002; Moghimi and Hamad, 2008; Yan et al., 2005), and cationic liposomes have long been known to induce complement activation (Chonn et al., 1991). Given that the central component of the complement system, C3, was among the most abundant proteins in the biomolecular corona of all liposomes, we finally also wanted to investigate how the complement system was involved in liposome clearance by blood leukocytes. Therefore, we again performed an inhibition experiment as described above, but this time using the 4W9A variant of the C3 inhibiting peptide compstatin, which prevents cleavage of C3 and hence prevents formation of the opsonin C3b (Mallik et al., 2005; Mastellos et al., 2015). In contrast to the inhibition experiments with CD44 and CD14, we observed an unchanged or increased uptake in the monocytes (Fig. 5c) but a reduced uptake in granulocytes (Fig. 5d) of the liposomes upon inhibition of C3. This even led to a

significant increase in monocyte specificity of the PEGylated TriArg liposomes (Supplementary Figure S20). Thus, the complement system is not directly involved in the monocyte targeting of the cationic liposomes, but it still affects their specificity as it is involved in the off-target uptake of the cationic liposomes in granulocytes. Since the overall liposome uptake in granulocytes is low (Fig. 1), this finding supports recent reports that the complement systems plays a minor role in liposome clearance by the MPS (Viana et al., 2020).

4. Conclusion

To investigate the monocyte-targeting mechanisms of cationic liposomes, we here conducted a comprehensive study involving both non-PEGylated and PEGylated cationic liposomes prepared with either DOTAP, POEPC or a triarginine lipopeptide. In agreement with our expectation, we found all of the liposomes to specifically target monocytes over other leukocytes in whole human blood. We also found that plasma factors were likely to mediate the targeting, prompting us to investigate the involvement of the biomolecular corona. The non-PEGylated liposomes were found to aggregate strongly in plasma, hence we only investigated the corona around the PEGylated liposomes. These liposomes were found to adsorb significant amounts of hyaluronan-associated proteins and proteoglycans, bringing us to investigate the involvement in the liposomal monocyte targeting of the TLR4 co-receptors CD44, recognising hyaluronan and several proteoglycans, and CD14, recognising the proteoglycan lumican. Separate inhibition of each of these receptors led to a marked decrease in monocyte targeting of the liposomes, possibly suggesting that both receptors are involved in a common uptake mechanism mediated via the TLR4 axis. In any case, we have identified two receptors involved in the monocyte targeting of cationic liposomes. This in turn suggests that proteoglycans and glycosaminoglycans may serve as opsonins for cationic liposomes, causing the liposomes to target monocytes. Our study thus represents an important step in deciphering the mechanism behind the monocyte-targeting capabilitity of cationic liposomes, demonstrating how a detailed analysis of the biomolecular corona can be used to gain such mechanistic insights. Future studies might be able to identify the specific proteoglycans or glycosaminoglycans involved in the monocyte targeting.

Overall, development of monocyte and macrophage targeting delivery platforms is important for immunotherapeutics, cancer therapy and treatments against autoimmune diseases, such as rheumatoid arthritis and atherosclerosis. The work presented here is an important step in understanding which biological mechanisms to take into account when developing new and improved delivery platforms for targeting monocytes to treat these diseases.

CRediT authorship contribution statement

Rasmus Münter: Writing – review & editing, Writing – original draft, Visualization, Validation, Project administration, Methodology, Investigation, Formal analysis, Data curation, Conceptualization. **Martin Bak:** Writing – review & editing, Visualization, Resources, Methodology, Investigation. **Mikkel E. Thomsen:** Writing – review & editing, Investigation, Formal analysis. **Ladan Parhamifar:** Writing – review & editing, Supervision, Methodology, Conceptualization. **Allan Stensballe:** Writing – review & editing, Supervision, Methodology, Funding acquisition. **Jens B. Simonsen:** Writing – review & editing, Supervision, Conceptualization. **Kasper Kristensen:** Writing – review & editing, Writing – original draft, Supervision, Methodology, Conceptualization. **Thomas L. Andresen:** Writing – review & editing, Supervision, Funding acquisition, Conceptualization.

Declaration of competing interest

The authors declare the following financial interests/personal relationships which may be considered as potential competing interests: Thomas L. Andresen and Ladan Parhamifar reports a relationship with MonTa Biosciences that includes: founding. Thomas L. Andresen, Ladan Parhamifar and Rasmus Münter have patent #WO2019012107 issued to Technical University of Denmark.

Data availability

Data will be made available on request.

Acknowledgement

We thank Katrine Jønsson and Anne Z. Eriksen for helping with blood drawing, Gael Clergeaud and Fredrik Melander for operating the ICP-MS, Casper Hempel for sharing his knowledge about glycosaminoglycans, and Jannik B. Larsen and Kasper B. Johnsen for critical feedback on the manuscript. The Lundbeck Foundation (Grant number R155-2013-14113), the European Research Council (Grant number ERC 310985), the Novo Nordisk Foundation (Grant number NNF16OC0022166), and the Danish Council for Independent Research (Grant number DFF 4184-00514) are gratefully acknowledged for funding. The Obelske Family Foundation, the Svend Andersen Foundation and the Spar Nord Foundation are acknowledged for grants to the LC-MS/MS analytical platform, enabling this study. The Danish Agency for Science and Higher Education is acknowledged for the funding to the Danish National Mass Spectrometry Platform for Functional Proteomics (PRO-MS; Grant no. 5072-00007B) enabling parts of this study.

Appendix A. Supplementary material

Supplementary data to this article can be found online at https://doi.org/10.1016/j.ijpharm.2024.124129.

References

Ahl, P.L., Bhatia, S.K., Meers, P., Roberts, P., Stevens, R., Dause, R., Perkins, W.R., Janoff, A.S., 1997. Enhancement of the in vivo circulation lifetime of L-α-distearoylphosphatidylcholine liposomes: importance of liposomal aggregation versus complement opsonization. Biochim. Biophys. Acta 1329, 370–382. https://doi.org/10.1016/S0005-2736(97)00129-6.

Akinc, A., Querbes, W., De, S., Qin, J., Frank-Kamenetsky, M., Jayaprakash, K.N., Jayaraman, M., Rajeev, K.G., Cantley, W.L., Dorkin, J.R., Butler, J.S., Qin, L., Racie, T., Sprague, A., Fava, E., Zeigerer, A., Hope, M.J., Zerial, M., Sah, D.W.Y., Fitzgerald, K., Tracy, M.A., Manoharan, M., Koteliansky, V., de Fougerolles, A., Maier, M.A., 2010. Targeted delivery of RNAi therapeutics with endogenous and exogenous ligand-based mechanisms. Mol. Ther. 18, 1357–1364. https://doi.org/10.1038/MT.2010.85.

Akinc, A., Maier, M.A., Manoharan, M., Fitzgerald, K., Jayaraman, M., Barros, S., Ansell, S., Du, X., Hope, M.J., Madden, T.D., Mui, B.L., Semple, S.C., Tam, Y.K., Ciufolini, M., Witzigmann, D., Kulkarni, J.A., van der Meel, R., Cullis, P.R., 2019. The Onpattro story and the clinical translation of nanomedicines containing nucleic acid-based drugs. Nat. Nanotechnol. 14, 1084–1087. https://doi.org/10.1038/s41565-019-0591-y.

Alam, S.B., Wang, F., Qian, H., Kulka, M., 2023. Apolipoprotein C3 facilitates internalization of cationic lipid nanoparticles into bone marrow-derived mouse mast cells. Sci. Rep. 13, 431. https://doi.org/10.1038/s41598-022-25737-7.

Allen, C., Dos Santos, N., Gallagher, R., Chiu, G.N.C., Shu, Y., Li, W.M., Johnstone, S.A., Janoff, A.S., Mayer, L.D., Webb, M.S., Bally, M.B., 2002. Controlling the Physical Behavior and Biological Performance of Liposome Formulations Through Use of Surface Grafted Poly(ethylene Glycol). Biosci. Rep. 22, 225–250. https://doi.org/10.1023/A:1020186505848.

Andresen, T.L., Jensen, S.S., Henriksen, J.R., Parhamifar, L., Lassen, R.M.M., 2019. Cationic liposomes. Patent no. WO2019012107.

Bennike, T.B., Kastaniegaard, K., Padurariu, S., Gaihede, M., Birkelund, S., Andersen, V., Stensballe, A., 2016. Comparing the proteome of snap frozen, RNAlater preserved, and formalin-fixed paraffin-embedded human tissue samples. EuPA Open Proteom. 10, 9–18. https://doi.org/10.1016/j.euprot.2015.10.001.

Bexborn, F., Engberg, A.E., Sandholm, K., Mollnes, T.E., Hong, J., Nilsson Ekdahl, K., 2009. Hirudin versus heparin for use in whole blood in vitro biocompatibility models. J. Biomed. Mater. Res. A 89, 951–959. https://doi.org/10.1002/jbm.a.32034.

Bi, Y., Chen, J., Hu, F., Liu, J., Li, M., Zhao, L., 2019. M2 Macrophages as a Potential Target for Antiatherosclerosis Treatment. Neural Plast. 2019, 6724903. https://doi.org/10.1155/2019/6724903.

Blanco, E., Shen, H., Ferrari, M., 2015. Principles of nanoparticle design for overcoming biological barriers to drug delivery. Nat. Biotechnol. 33, 941–951. https://doi.org/10.1038/nbt.3330.
Bobryshev, Y.V., Ivanova, E.A., Chistiakov, D.A., Nikiforov, N.G., Orekhov, A.N., 2016. Macrophages and Their Role in Atherosclerosis: Pathophysiology and Transcriptome Analysis. Biomed Res. Int. 2016, 9582430. https://doi.org/10.1155/2016/9582430.
Bozzuto, G., Molinari, A., 2015. Liposomes as nanomedical devices. Int. J. Nanomed. 10, 975–999. https://doi.org/10.2147/IJN.S68861.
Cao, D., Luo, J., Chen, D., Xu, H., Shi, H., Jing, X., Zang, W., 2016. CD36 regulates lipopolysaccharide-induced signaling pathways and mediates the internalization of Escherichia coli in cooperation with TLR4 in goat mammary gland epithelial cells. Sci. Rep. 6, 23132. https://doi.org/10.1038/srep23132.
Cedrone, E., Neun, B.W., Rodriguez, J., Vermilya, A., Clogston, J.D., McNeil, S.E., Barenholz, Y., Szebeni, J., Dobrovolskaia, M., 2018. Anticoagulants Influence the Performance of In Vitro Assays Intended for Characterization of Nanotechnology-Based Formulations. Molecules 23, 12. https://doi.org/10.3390/molecules23010012.
Chonn, A., Cullis, P.R., Devine, D.V., 1991. The role of surface charge in the activation of the classical and alternative pathways of complement by liposomes. J. Immunol. 146, 4234–4241. https://doi.org/10.4049/jimmunol.146.12.4234.
Corbo, C., Molinaro, R., Parodi, A., Toledano Furman, N.E., Salvatore, F., Tasciotti, E., 2016. The impact of nanoparticle protein corona on cytotoxicity, immunotoxicity and target drug delivery. Nanomedicine 11, 81–100. https://doi.org/10.2217/nnm.15.188.
Cox, J., Hein, M.Y., Luber, C.A., Paron, I., Nagaraj, N., Mann, M., 2014. Accurate Proteome-wide Label-free Quantification by Delayed Normalization and Maximal Peptide Ratio Extraction, Termed MaxLFQ. Mol. Cell. Proteomics 13, 2513–2526. https://doi.org/10.1074/mcp.M113.031591.
Danielson, B.T., Knudson, C.B., Knudson, W., 2015. Extracellular Processing of the Cartilage Proteoglycan Aggregate and Its Effect on CD44-mediated Internalization of Hyaluronan. J. Biol. Chem. 290, 9555–9570. https://doi.org/10.1074/jbc.M115.643171.
de Lázaro, I., Mooney, D.J., 2021. Obstacles and opportunities in a forward vision for cancer nanomedicine. Nat. Mater. 20, 1469–1479. https://doi.org/10.1038/s41563-021-01047-7.
Dow, S., 2008. Liposome–nucleic acid immunotherapeutics. Expert Opin. Drug Deliv. 5, 11–24. https://doi.org/10.1517/17425247.5.1.11.
Dowling, D.J., 2018. Recent Advances in the Discovery and Delivery of TLR7/8 Agonists as Vaccine Adjuvants. Immunohorizons 2, 185–197. https://doi.org/10.4049/immunohorizons.1700063.
Embry, J.J., Knudson, W., 2003. G1 domain of aggrecan cointernalizes with hyaluronan via a CD44-mediated mechanism in bovine articular chondrocytes. Arthritis Rheum. 48, 3431–3441. https://doi.org/10.1002/art.11323.
Fadok, V.A., Warner, M.L., Bratton, D.L., Henson, P.M., 1998. CD36 is required for phagocytosis of apoptotic cells by human macrophages that use either a phosphatidylserine receptor or the vitronectin receptor ($\alpha_v\beta_3$). J. Immunol. 161, 6250–6257.
Filion, M.C., Phillips, N.C., 1997. Toxicity and immunomodulatory activity of liposomal vectors formulated with cationic lipids toward immune effector cells. Biochim. Biophys. Acta 1329, 345–356. https://doi.org/10.1016/S0005-2736(97)00126-0.
Frey, H., Schroeder, N., Manon-Jensen, T., Iozzo, R.V., Schaefer, L., 2013. Biological interplay between proteoglycans and their innate immune receptors in inflammation. FEBS J. 280, 2165–2179. https://doi.org/10.1111/febs.12145.
Fries, E., Kaczmarczyk, A., 2003. Inter-alpha-inhibitor, hyaluronan and inflammation. Acta Biochim. Pol. 50, 735–742. https://doi.org/10.18388/abp.2003_3664.
Fujimoto, T., Kawashima, H., Tanaka, T., Hirose, M., Toyama-Sorimachi, N., Matsuzawa, Y., Miyasaka, M., 2001. CD44 binds a chondroitin sulfate proteoglycan, aggrecan. Int. Immunol. 13, 359–366. https://doi.org/10.1093/intimm/13.3.359.
Fukui, S., Iwamoto, N., Takatani, A., Igawa, T., Shimizu, T., Umeda, M., Nishino, A., Horai, Y., Hirai, Y., Koga, T., Kawashiri, S., Tamai, M., Ichinose, K., Nakamura, H., Origuchi, T., Masuyama, R., Kosai, K., Yanagihara, K., Kawakami, A., 2018. M1 and M2 Monocytes in Rheumatoid Arthritis: A Contribution of Imbalance of M1/M2 Monocytes to Osteoclastogenesis. Front. Immunol. 8, 1958. https://doi.org/10.3389/fimmu.2017.01958.
Goodison, S., Urquidi, V., Tarin, D., 1999. CD44 cell adhesion molecules. Mol. Pathol. 52, 189–196. https://doi.org/10.1136/mp.52.4.189.
Guerriero, J.L., 2018. Macrophages: The Road Less Traveled, Changing Anticancer Therapy. Trends Mol. Med. 24, 472–489. https://doi.org/10.1016/j.molmed.2018.03.006.
Harris, E., Weigel, P.H., 2009. Functional Aspects of the Hyaluronan and Chondroitin Sulfate Receptors. In: Animal Lectins: A Functional View. CRC Press, pp. 171–192. https://doi.org/10.1201/9781420006971.ch12.
Horvatinovich, J.M., Grogan, E.W., Norris, M., Steinkasserer, A., Lemos, H., Mellor, A.L., Tcherepanova, I.Y., Nicolette, C.A., DeBenedette, M.A., 2017. Soluble CD83 Inhibits T Cell Activation by Binding to the TLR4/MD-2 Complex on CD14$^+$ Monocytes. J. Immunol. 198, 2286–2301. https://doi.org/10.4049/jimmunol.1600802.
Isacke, C.M., Yarwood, H., 2002. The hyaluronan receptor, CD44. Int. J. Biochem. Cell Biol. 34, 718–721. https://doi.org/10.1016/s1357-2725(01)00166-2.
Ishida, T., Harashima, H., Kiwada, H., 2002. Liposome Clearance. Biosci. Rep. 22, 197–224. https://doi.org/10.1023/A:1020134521778.
Iwasa, A., Akita, H., Khalil, I., Kogure, K., Futaki, S., Harashima, H., 2006. Cellular uptake and subsequent intracellular trafficking of R8-liposomes introduced at low temperature. Biochim. Biophys. Acta 1758, 713–720. https://doi.org/10.1016/j.bbamem.2006.04.015.
Javaid, N., Yasmeen, F., Choi, S., 2019. Toll-like receptors and relevant emerging therapeutics with reference to delivery methods. Pharmaceutics 11, 441. https://doi.org/10.3390/pharmaceutics11090441.
Johansen, P.T., Zucker, D., Parhamifar, L., Pourhassan, H., Madsen, D.V., Henriksen, J. R., Gad, M., Barberis, A., Maj, R., Andresen, T.L., Jensen, S.S., 2015. Monocyte targeting and activation by cationic liposomes formulated with a TLR7 agonist. Expert Opin. Drug Deliv. 12, 1045–1058. https://doi.org/10.1517/17425247.2015.1009444.
Ju, Y., Kelly, H.G., Dagley, L.F., Reynaldi, A., Schlub, T.E., Spall, S.K., Bell, C.A., Cui, J., Mitchell, A.J., Lin, Z., Wheatley, A.K., Thurecht, K.J., Davenport, M.P., Webb, A.I., Caruso, F., Kent, S.J., 2020. Person-Specific Biomolecular Coronas Modulate Nanoparticle Interactions with Immune Cells in Human Blood. ACS Nano 14, 15723–15737. https://doi.org/10.1021/acsnano.0c06679.
Karathanasis, E., Geigerman, C.M., Parkos, C.A., Chan, L., Bellamkonda, R.V., Jaye, D.L., 2009. Selective targeting of nanocarriers to neutrophils and monocytes. Ann. Biomed. Eng. 37, 1984–1992. https://doi.org/10.1007/s10439-009-9702-5.
Kawashima, H., Hirose, M., Hirose, J., Nagakubo, D., Plaas, A.H.K., Miyasaka, M., 2000. Binding of a Large Chondroitin Sulfate/Dermatan Sulfate Proteoglycan, Versican, to L-selectin, P-selectin, and CD44. J. Biol. Chem. 275, 35448–35456. https://doi.org/10.1074/jbc.M003387200.
Kelly, C., Jefferies, C., Cryan, S.-A., 2011. Targeted Liposomal Drug Delivery to Monocytes and Macrophages. J. Drug Deliv. 2011, 727241. https://doi.org/10.1155/2011/727241.
Klauber, T.C.B., Laursen, J.M., Zucker, D., Brix, S., Jensen, S.S., Andresen, T.L., 2017. Delivery of TLR7 agonist to monocytes and dendritic cells by DCIR targeted liposomes induces robust production of anti-cancer cytokines. Acta Biomater. 53, 367–377. https://doi.org/10.1016/j.actbio.2017.01.072.
Knudsen, K.B., Northeved, H., Kumar, P.E.K., Permin, A., Gjetting, T., Andresen, T.L., Larsen, S., Wegener, K.M., Lykkesfeldt, J., Jantzen, K., Loft, S., Møller, P., Roursgaard, M., 2015. In vivo toxicity of cationic micelles and liposomes. Nanomedicine 11, 467–477. https://doi.org/10.1016/J.NANO.2014.08.004.
Korsholm, K.S., Agger, E.M., Foged, C., Christensen, D., Dietrich, J., Andersen, C.S., Geisler, C., Andersen, P., 2007. The adjuvant mechanism of cationic dimethyldioctadecylammonium liposomes. Immunology 121, 216–226. https://doi.org/10.1111/j.1365-2567.2007.02560.x.
Kristensen, K., Engel, T.B., Stensballe, A., Simonsen, J.B., Andresen, T.L., 2019. The hard protein corona of stealth liposomes is sparse. J. Control. Release 307, 1–15. https://doi.org/10.1016/j.jconrel.2019.05.042.
Kristensen, K., Münter, R., Kempen, P.J., Thomsen, M.E., Stensballe, A., Andresen, T.L., 2021. Isolation methods commonly used to study the liposomal protein corona suffer from contamination issues. Acta Biomater. 130, 460–472. https://doi.org/10.1016/j.actbio.2021.06.008.
Li, W., Szoka, F.C., 2007. Lipid-based Nanoparticles for Nucleic Acid Delivery. Pharm. Res. 24, 438–449. https://doi.org/10.1007/s11095-006-9180-5.
Lonez, C., Vandenbranden, M., Ruysschaert, J.-M., 2008. Cationic liposomal lipids: From gene carriers to cell signaling. Prog. Lipid Res. 47, 340–347. https://doi.org/10.1016/j.plipres.2008.03.002.
Mallick, S., Choi, J.S., 2014. Liposomes: Versatile and Biocompatible Nanovesicles for Efficient Biomolecules Delivery. J. Nanosci. Nanotechnol. 14, 755–765. https://doi.org/10.1166/jnn.2014.9080.
Mallik, B., Katragadda, M., Spruce, L.A., Carafides, C., Tsokos, C.G., Morikis, D., Lambris, J.D., 2005. Design and NMR Characterization of Active Analogues of Compstatin Containing Non-Natural Amino Acids. J. Med. Chem. 48, 274–286. https://doi.org/10.1021/jm0495531.
Mastellos, D.C., Yancopoulou, D., Kokkinos, P., Huber-Lang, M., Hajishengallis, G., Biglarnia, A.R., Lupu, F., Nilsson, B., Risitano, A.M., Ricklin, D., Lambris, J.D., 2015. Compstatin: a C3-targeted complement inhibitor reaching its prime for bedside intervention. Eur. J. Clin. Invest. 45, 423–440. https://doi.org/10.1111/eci.12419.
McDonald, B., Kubes, P., 2015. Interactions between CD44 and Hyaluronan in Leukocyte Trafficking. Front. Immunol. 6 (68) https://doi.org/10.3389/fimmu.2015.00068.
Moghimi, S.M., Hamad, I., 2008. Liposome-Mediated Triggering of Complement Cascade. J. Liposome Res. 18, 195–209. https://doi.org/10.1080/08982100802309552.
Moore, T.L., Rodriguez-Lorenzo, L., Hirsch, V., Balog, S., Urban, D., Jud, C., Rothen-Rutishauser, B., Lattuada, M., Petri-Fink, A., 2015. Nanoparticle colloidal stability in cell culture media and impact on cellular interactions. Chem. Soc. Rev. 44, 6287–6305. https://doi.org/10.1039/c4cs00487f.
Münter, R., Bak, M., Christensen, E., Kempen, P.J., Larsen, J.B., Kristensen, K., Parhamifar, L., Andresen, T.L., 2022a. Mechanisms of selective monocyte targeting by liposomes functionalized with a cationic, arginine-rich lipopeptide. Acta Biomater. 144, 96–108. https://doi.org/10.1016/j.actbio.2022.03.029.
Münter, R., Simonsen, J.B., 2023. Comment on “Optimal centrifugal isolating of liposome–protein complexes from human plasma” by L. Digiacomo, F. Giulimondi, A. L. Capriotti, S. Piovesana, C. M. Montone, R. Z. Chiozzi, A. Laganá, M. Mahmoudi, D. Pozzi and G. Caracciolo, Nanoscale Adv., 2021, 3, 3824. Nanoscale Adv. 5, 290–299. https://doi.org/10.1039/D2NA00343K.
Münter, R., Stavnsbjerg, C., Christensen, E., Thomsen, M.E., Stensballe, A., Hansen, A.E., Parhamifar, L., Kristensen, K., Simonsen, J.B., Larsen, J.B., Andresen, T.L., 2022b. Unravelling Heterogeneities in Complement and Antibody Opsonization of Individual Liposomes as a Function of Surface Architecture. Small 18, e2106529. https://doi.org/10.1002/smll.202106529.
Muto, J., Yamasaki, K., Taylor, K.R., Gallo, R.L., 2009. Engagement of CD44 by hyaluronan suppresses TLR4 signaling and the septic response to LPS. Mol. Immunol. 47, 449–456. https://doi.org/10.1016/j.molimm.2009.08.026.
Nishino, M., Matsuzaki, I., Musangile, F.Y., Takahashi, Y., Iwahashi, Y., Warigaya, K., Kinoshita, Y., Kojima, F., Murata, S.-I., 2020. Measurement and visualization of cell

membrane surface charge in fixed cultured cells related with cell morphology. PLoS One 15, e0236373. https://doi.org/10.1371/JOURNAL.PONE.0236373.
Ong, Y.R., De Rose, R., Johnston, A.P.R., 2021. In Vivo Quantification of Nanoparticle Association with Immune Cell Subsets in Blood. Adv. Healthc. Mater. 10, 2002160. https://doi.org/10.1002/adhm.202002160.
Pedersbæk, D., Jønsson, K., Madsen, D.V., Weller, S., Bohn, A.B., Andresen, T.L., Simonsen, J.B., 2020. A quantitative ex vivo study of the interactions between reconstituted high-density lipoproteins and human leukocytes. RSC Adv. 10, 3884–3894. https://doi.org/10.1039/C9RA08203D.
Petrey, A.C., de la Motte, C.A., 2014. Hyaluronan, a Crucial Regulator of Inflammation. Front. Immunol. 5, 101. https://doi.org/10.3389/fimmu.2014.00101.
Płóciennikowska, A., Hromada-Judycka, A., Borzęcka, K., Kwiatkowska, K., 2015. Co-operation of TLR4 and raft proteins in LPS-induced pro-inflammatory signaling. Cell. Mol. Life Sci. 72, 557–581. https://doi.org/10.1007/s00018-014-1762-5.
Ramana, L.N., Sharma, S., Sethuraman, S., Ranga, U., Krishnan, U.M., 2012. Investigation on the stability of saquinavir loaded liposomes: Implication on stealth, release characteristics and cytotoxicity. Int. J. Pharm. 431, 120–129. https://doi.org/10.1016/j.ijpharm.2012.04.054.
Ruffell, B., Poon, G.F.T., Lee, S.S.M., Brown, K.L., Tjew, S.-L., Cooper, J., Johnson, P., 2011. Differential Use of Chondroitin Sulfate to Regulate Hyaluronan Binding by Receptor CD44 in Inflammatory and Interleukin 4-activated Macrophages. J. Biol. Chem. 286, 19179–19190. https://doi.org/10.1074/jbc.M110.200790.
Ruozi, B., Forni, F., Battini, R., Vandelli, M.A., 2003. Cationic Liposomes for Gene Transfection. J. Drug Target. 11, 407–414. https://doi.org/10.1080/10611860310001655600.
Schöttler, S., Klein, K., Landfester, K., Mailänder, V., 2016. Protein source and choice of anticoagulant decisively affect nanoparticle protein corona and cellular uptake. Nanoscale 8, 5526–5536. https://doi.org/10.1039/C5NR08196C.
Schütt, C., 1999. CD14. Int. J. Biochem. Cell Biol. 31, 545–549. https://doi.org/10.1016/S1357-2725(98)00153-8.
Schwanhäusser, B., Busse, D., Li, N., Dittmar, G., Schuchhardt, J., Wolf, J., Chen, W., Selbach, M., 2011. Global quantification of mammalian gene expression control. Nature 473, 337–342. https://doi.org/10.1038/nature10098.
Senbanjo, L.T., Chellaiah, M.A., 2017. CD44: A Multifunctional Cell Surface Adhesion Receptor Is a Regulator of Progression and Metastasis of Cancer Cells. Front. Cell Dev. Biol. 5, 18. https://doi.org/10.3389/fcell.2017.00018.
Shao, H., Lee, S., Gae-Scott, S., Nakata, C., Chen, S., Hamad, A.R., Chakravarti, S., 2012. Extracellular Matrix Lumican Promotes Bacterial Phagocytosis, and Lum$^{-/-}$ Mice Show Increased Pseudomonas aeruginosa Lung Infection Severity. J. Biol. Chem. 287, 35860–35872. https://doi.org/10.1074/jbc.M112.380550.
Shaw, M.T., 1980. Monocytic leukemias. Hum. Pathol. 11, 215–227. https://doi.org/10.1016/S0046-8177(80)80003-7.
Silverstein, R.L., Febbraio, M., 2009. CD36, a scavenger receptor involved in immunity, metabolism, angiogenesis, and behavior. Sci. Signal. 2, re3. https://doi.org/10.1126/scisignal.272re3.
Smits, E.L.J.M., Ponsaerts, P., Berneman, Z.N., Van Tendeloo, V.F.I., 2008. The Use of TLR7 and TLR8 Ligands for the Enhancement of Cancer Immunotherapy. Oncologist 13, 859–875. https://doi.org/10.1634/theoncologist.2008-0097.
Stewart, C.R., Stuart, L.M., Wilkinson, K., van Gils, J.M., Deng, J., Halle, A., Rayner, K.J., Boyer, L., Zhong, R., Frazier, W.A., Lacy-Hulbert, A., El Khoury, J., Golenbock, D.T., Moore, K.J., 2010. CD36 ligands promote sterile inflammation through assembly of a Toll-like receptor 4 and 6 heterodimer. Nat. Immunol. 11, 155–161. https://doi.org/10.1038/ni.1836.
Underhill, C., 1992. CD44: the hyaluronan receptor. J. Cell Sci. 103, 293–298. https://doi.org/10.1242/jcs.103.2.293.
Vachon, E., Martin, R., Plumb, J., Kwok, V., Vandivier, R.W., Glogauer, M., Kapus, A., Wang, X., Chow, C.-W., Grinstein, S., Downey, G.P., 2006. CD44 is a phagocytic receptor. Blood 107, 4149–4158. https://doi.org/10.1182/blood-2005-09-3808.
Viana, I.M.O., Grenier, P., Defrêne, J., Barabé, F., Lima, E.M., Bertrand, N., 2020. Role of the complement cascade in the biological fate of liposomes in rodents. Nanoscale 12, 18875–18884. https://doi.org/10.1039/D0NR04100A.
Walkey, C.D., Chan, W.C.W., 2012. Understanding and controlling the interaction of nanomaterials with proteins in a physiological environment. Chem. Soc. Rev. 41, 2780–2799. https://doi.org/10.1039/C1CS15233E.
Walkey, C.D., Olsen, J.B., Song, F., Liu, R., Guo, H., Olsen, D.W.H., Cohen, Y., Emili, A., Chan, W.C.W., 2014. Protein Corona Fingerprinting Predicts the Cellular Interaction of Gold and Silver Nanoparticles. ACS Nano 8, 2439–2455. https://doi.org/10.1021/nn406018q.
Wu, F., Vij, N., Roberts, L., Lopez-Briones, S., Joyce, S., Chakravarti, S., 2007. A Novel Role of the Lumican Core Protein in Bacterial Lipopolysaccharide-induced Innate Immune Response. J. Biol. Chem. 282, 26409–26417. https://doi.org/10.1074/jbc.M702402200.
Yan, X., Scherphof, G.L., Kamps, J.A.A.M., 2005. Liposome Opsonization. J. Liposome Res. 15, 109–139. https://doi.org/10.1081/LPR-64971.
Zanoni, I., Ostuni, R., Marek, L.R., Barresi, S., Barbalat, R., Barton, G.M., Granucci, F., Kagan, J.C., 2011. CD14 Controls the LPS-Induced Endocytosis of Toll-like Receptor 4. Cell 147, 868–880. https://doi.org/10.1016/j.cell.2011.09.051.
Zhao, W., Zhuang, S., Qi, X.-R., 2011. Comparative study of the in vitro and in vivo characteristics of cationic and neutral liposomes. Int. J. Nanomedicine 6, 3087–3098. https://doi.org/10.2147/IJN.S25399.
Zhuo, L., Kimata, K., 2008. Structure and Function of Inter-α-Trypsin Inhibitor Heavy Chains. Connect. Tissue Res. 49, 311–320. https://doi.org/10.1080/03008200802325458.